Biochimica et Biophysica Acta 1798 (2010) 40–51

Contents lists available at ScienceDirect

Biochimica et Biophysica Acta

journal homepage: www.elsevier.com/locate/bbamem

Structural and thermodynamic determinants of chain-melting transition temperatures for phospholipid and glycolipids membranes

Derek Marsh

Max-Planck-Institut für biophysikalische Chemie, Abteilung Spektroskopie und photochemische Kinetik, 37070 Göttingen, Germany

ARTICLE INFO

Article history:
Received 2 September 2009
Received in revised form 7 October 2009
Accepted 14 October 2009
Available online 22 October 2009

Keywords:
Lipid bilayer
Chain melting
Chain asymmetry
Chain unsaturation
Chain interdigitation
Branched chain
Headgroup length

ABSTRACT

For optimum function, biological membranes need a fluid environment, which is afforded by the liquid-disordered phase of lipids with low chain-melting temperatures or the liquid-ordered phase that is formed by combining high chain-melting lipids with cholesterol. The dependence of chain-melting transition temperature on lipid chain structure is therefore of central importance. The currently available database, including sphingolipids and glycolipids, is summarised here by parameterising systematic dependences on molecular structure in terms of suitable thermodynamic models. Chain-length dependence, chain asymmetry of lipids forming partially interdigitated and mixed interdigitated gel phases, chain unsaturation, positional dependence of methyl branching, headgroup-attached and α-branched chains, and length of zwitterionic headgroups are all covered. This type of information is essential for biophysical approaches to functional lipidomics.

1. Introduction

Biological membranes require a fluid lipid environment for optimal activity of membrane-bound enzymes and transport systems [1–7], and for the necessary elastic membrane flexibility [8–10]. This is generally achieved by lipids with low chain-melting transitions. However, different states of fluidity offer the organizational advantage of in-plane compartmentation, as by the formation of lipid-raft domains in plasma membranes [11]. The latter are produced by combining a high-melting lipid with cholesterol, resulting in formation of the so-called liquid-ordered phase [12].

The chain-melting transition temperature therefore assumes an important role in the lipid composition of biological membranes. In the present paper, I review the dependences of membrane chain-melting temperature on structure of the phospholipid chains. This information is crucial to the biophysical aspects of any functional lipidomics initiative. The approach is to use thermodynamic models [13–16], which results in a convenient parameterization of the systematic dependences of chain-melting temperature on chain structure. Optimised parameters are given which summarise the currently available database. In addition to extending existing analyses to cover new data, asymmetry of lipids forming mixed interdigitated gel phases, the positional dependence of methyl chain branches, headgroup length of zwitterionic lipids, and chain asymmetry of sphingomyelins are treated here for the first time.

Biological membrane lipids are chosen to have chains of sufficient length to ensure maintenance of the essential barrier properties of the membrane and to provide hydrophobic matching with embedded membrane-spanning proteins, whilst fulfilling the requirements for chain-melting temperature that are outlined above.

2. Chain-melting transition

At a first-order transition, the Gibbs free energy is continuous, but there are discontinuous changes, ΔH_t and ΔS_t, in enthalpy and entropy:

$$\Delta G_t = \Delta H_t - T_t \Delta S_t = 0 \tag{1}$$

where subscript "*t*" indicates changes taking place at the transition temperature, T_t. The transition temperature is therefore related to the calorimetric properties by:

$$T_t = \frac{\Delta H_t}{\Delta S_t} \tag{2}$$

Hence, it is the dependence of the transition enthalpy and transition entropy on lipid chain structure that determines the chain dependence of the transition temperature.

E-mail address: dmarsh@gwdg.de.

0005-2736/$ – see front matter © 2009 Elsevier B.V. All rights reserved.
doi:10.1016/j.bbamem.2009.10.010

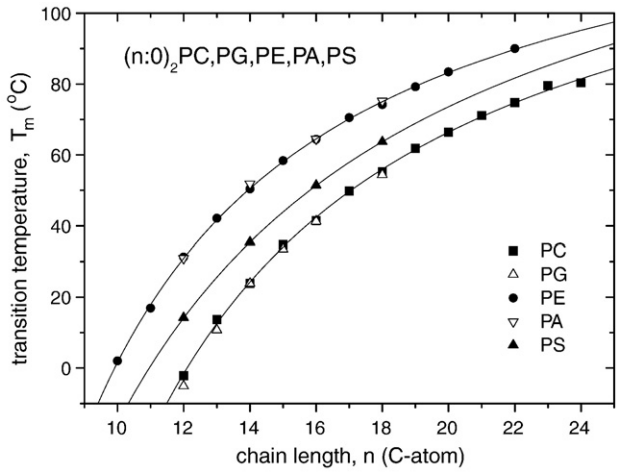

Fig. 1. Chain-length dependence of the chain-melting transition temperature for bilayer membranes of saturated, symmetrical straight-chain diacyl phospholipids: Phosphatidylcholine (solid squares, PC, [18–20]), phosphatidylethanolamine (solid circles, PE, [21,22]), phosphatidylglycerol (open triangles, PG, [23]); phosphatidylserine (solid triangles, PS, [24]), phosphatidic acid (open inverted triangles, PA, [25]). Solid lines are non-linear, least-squares fits of Eq. (5) to the data for PC, PE and PS. Fitting parameters are given in Table 1.

3. Chain-length dependence

For two-chain lipids with zero or constant chain asymmetry, the transition enthalpy and transition entropy are found to depend linearly on lipid chain length, n [13,17]:

$$\Delta H_t(n) = \Delta H_{inc}(n - n_H) \tag{3}$$

$$\Delta S_t(n) = \Delta S_{inc}(n - n_S) \tag{4}$$

where ΔH_{inc} and ΔS_{inc} are the incremental transition enthalpy and transition entropy per CH_2 group, respectively, and n_H and n_S are the chain lengths for which the transition enthalpy and transition entropy, respectively, extrapolate to zero, which account for all end contributions. These end contributions are given simply by: $\Delta H_{end} = n_H \Delta H_{inc}$ for the transition enthalpy, and $\Delta S_{end} = n_S \Delta S_{inc}$ for the transition entropy. Not only do they include contributions from the polar head groups, chain linkage and terminal methyl groups, but they also can include inherent chain asymmetries, branched chains and ω-cyclohexyl groups, provided that these are maintained constant with increasing chain length, as for instance in a homologous series of isoacyl or anteisoacyl chains.

From Eqs. (2)–(4), the chain-length dependence of the transition temperature for two-chain lipids with zero or constant chain asymmetry is given by:

$$T_t(n) = T_t^{\infty}\left(1 - \frac{n_H - n_S}{n - n_S}\right) \tag{5}$$

where $T_t^{\infty}(\equiv \Delta H_{inc}/\Delta S_{inc})$ is the transition temperature extrapolated to infinite chain length. Equation 5 is found to describe very well the dependence of the chain-melting temperature, T_m, on chain length for a wide variety of bilayer-forming diacyl and dialkyl phospholipids, and over a considerable range of n (see, e.g., Fig. 1). Table 1

Table 1
Parameters describing the dependence of the chain-melting transition temperatures of lipid bilayers on chain length for lipids with symmetrical, saturated chains, according to Eq. (5).

Lipid[a]	n	T_m^{∞} (K)	$n_H - n_S$	n_S	Refs.[b]
1,2-(n:0)$_2$PC	12–24	420.8 ± 4.1	3.39 ± 0.24	2.44 ± 0.55	[18–20]
1,2-(n:0$_i$)$_2$PC	12–22	422.6 ± 3.9	3.97 ± 0.20	3.13 ± 0.36	[26,27]
1,2-(n:0$_{ai}$)$_2$PC	12–22	423.6 ± 7.0	5.08 ± 0.42	0.55 ± 0.74	[28]
1,2-(2Me-n:0)$_2$PC	14–20	407.9 ± 9.2	2.74 ± 0.43	5.48 ± 0.95	[29]
1,2-(n:0$_{dmi}$)$_2$PC odd n	15–21	401.9 ± 18.2	4.28 ± 1.17	2.56 ± 2.35	[30]
even n	14–22	407.5 ± 4.7	4.11 ± 0.25	4.17 ± 0.46	[30]
1,2-($\omega_{ch}n$:0)$_2$PC odd n	9–17	403.1 ± 8.9	3.10 ± 0.48	−0.15 ± 1.04	[31]
even n	10–18	425.4 ± 7.0	3.98 ± 0.38	−0.38 ± 0.74	[31]
1,2-(O-n:0)$_2$PC	12–18	404.2 ± 1.5	2.67 ± 0.07	3.67 ± 0.16	[32]
1,2-(n:0)$_2$PE	10–22	422.0 ± 2.3	2.81 ± 0.12	1.96 ± 0.28	[21,22]
1,2-(n:0$_i$)$_2$PE	17–20	371.7 ± 1.9	0.720 ± 0.056	12.24 ± 0.24	[33]
1,2-(O-n:0)$_2$PE	12–18	396.0 ± 2.0	1.45 ± 0.08	5.47 ± 0.26	[17]
1,2-(n:0)$_2$PG[c]	12–18	396.6 ± 4.0	2.27 ± 0.16	5.01 ± 0.37	[23]
1,2-(n:0)$_2$PS[d]	12–18	435.5 ± 1.8	4.06 ± 0.10	0.06 ± 0.21	[24]
1,2-(n:0)$_2$PA[e]	12–18	407.5 ± 12.7	2.06 ± 0.60	3.86 ± 1.64	[25]
1,2-(n:0)$_2$PEMe	11–17	426.7 ± 8.1	3.33 ± 0.41	1.15 ± 0.85	[34–37]
1,2-(n:0)$_2$PE(N-n:0) 0 M NaCl	12–18	421.7 ± 7.1	2.90 ± 0.39	1.44 ± 0.98	[38]
1 M NaCl		428.9 ± 22.0	3.16 ± 1.28	0.59 ± 3.12	[38]
1,2-(n:0)$_2$GlcαDG	11–20	408.5 ± 4.5	2.30 ± 0.21	3.94 ± 0.50	[39]
1,2-(n:0$_i$)$_2$GlcαDG	13–19	442.2 ± 14.4	4.43 ± 0.78	1.39 ± 1.45	[86]
1,2-(n:0)$_2$GlcβDG	12–20	422.2 ± 6.6	2.94 ± 0.37	1.98 ± 0.91	[40]
1,2-(n:0)$_2$GalβDG	10–20	409.6 ± 4.0	2.24 ± 0.17	3.59 ± 0.40	[41]
1,2-(O-n:0)$_2$GlcβDG	10–18	404.4 ± 5.5	2.13 ± 0.24	3.29 ± 0.56	[42]
rac-(O-n:0)$_2$GlcβDG[f]	10–20	401.4 ± 1.6	1.99 ± 0.07	3.60 ± 0.19	[87]
1,2-(O-n:0)$_2$GalβDG	12–18	379.0 ± 4.4	1.01 ± 0.16	6.84 ± 0.59	[43]
rac-(O-n:0)$_2$GalβDG[f]	10–18	404.0 ± 1.9	1.99 ± 0.08	3.74 ± 0.21	[88]

[a] *Chain notation*: (17:0i) ≡ (15Me-16:0): isoheptadecanoyl ≡ 15-methylhexadecanoyl; (17:0$_{ai}$) ≡ (14Me-16:0): anteisoheptadecanoyl ≡ 14-methylhexadecanoyl; (2Me-16:0): 2-methylhexadecanoyl; (14:0$_{dmi}$) ≡ (11Me$_2$-12:0): dimethylisotetradecanoyl ≡ 11,11-dimethyldodecanoyl (≡ ω-*t*-butyl-decanoyl); (ω$_{ch}$13:0): ω-cyclohexyl-tridecanoyl (19 C-atoms). *Headgroup notation*: PC, phosphatidylcholine; PE, phosphatidylethanolamine; PG, phosphatidylglycerol; PS, phosphatidylserine; PA, phosphatidic acid; PEMe, *N*-methyl phosphatidylethanolamine; PE(*N*-*n*:0), *N*-acyl phosphatidylethanolamine; GlcαDG: 1,2-diacyl-3-α-D-glucosyl-*sn*-glycerol; GlcβDG: 1,2-diacyl-3-β-D-glucosyl-*sn*-glycerol GalβDG: 1,2-diacyl-3-β-D-galactosyl-*sn*-glycerol.

[b] References to experimental data used in fitting. For 1,2-(n:0$_i$)$_2$PC, 1,2-(n:0$_{dmi}$)$_2$PC, 1,2-($\omega_{ch}n$:0)$_2$PC, 1,2-(n:0$_i$)$_2$PE, 1,2-(O-n:0)$_2$PE, 1,2-(n:0)$_2$GlcαDG and 1,2-(n:0)$_2$GlcβDG, the data sets and fitting parameters are the same as given in the original analysis of ref. [13]. For 1,2-(n:0)$_2$PC and 1,2-(n:0)$_2$PE, the data sets are extended and fitting parameters differ slightly from those given originally [13]. For 1,2-(n:0$_{ai}$)$_2$PC, the same data set is used, but the fit is better than in ref. [13]. For 1,2-(O-n:0)$_2$PC, an incomplete data set was used originally; the present fitting parameters supersede those in ref. [13].

[c] In 0.1 M NaCl, 50 mM Tris, 10 mM EDTA (pH 7.4).

[d] In 0.15 M NaCl, 50 mM Tris, 5 mM EDTA, 2 mM NaN_3 (pH 7.4).

[e] In 5 mM K_2PO_4, 5 mM EDTA (pH 7.0).

[f] Glycerol backbone is racemic mixture.

summarises non-linear, least-squares fitting parameters of Eq. (5), for the entire database.

In Table 1, the values of T_m^∞ are much the same, in the region of 400–420 K (~130–150 °C), for all lipids. This is to be expected because T_m^∞ is the extrapolated limit for very long chains, where contributions from end effects become relatively insignificant compared with the chain contributions. On the other hand, the values of n_H and n_S reflect the differences in enthalpic and entropic contributions from the various lipid head groups for a given type of chain, and the different types of chain or chain linkage for a given polar head group. Note that, because the branched methyl groups are included in the total chainlength n of isoacyl and anteisoacyl lipids, their values of n_H and n_S should be reduced by one for n:0_i and n:0_{ai} chains, and by two for n:0_{dmi} chains, when comparing structurally with the corresponding n:0 straight-chain lipids. This correction clearly is not required for the differences, $n_H - n_S$, that are listed in Table 1. Correspondingly, the terminal cyclohexyl group is not included in the total chain length, n, of the $\omega_{cy}n$:0 lipids, which accounts in part for why these lipids have the lowest values of n_S in Table 1.

4. Chain asymmetry—partial interdigitation

For two-chain lipids with asymmetrical chains of constant mean length, $n = (n_1 + n_2)/2$, where n_1 and n_2 are the numbers of C-atoms in the *sn*-1 and *sn*-2 chains, respectively, the chain-melting enthalpy and entropy have a bilinear dependence on the chain length asymmetry, $\Delta n = n_1 - n_2$, that reaches a maximum for an asymmetry, Δn_o, that corresponds to the conformational inequivalence of the *sn*-1 and *sn*-2 chains [14]. This holds for intermediate degrees of asymmetry, such that interdigitation of chains from apposing bilayer leaflets in the gel phase is only partial (see Fig. 2). As will be seen below in Section 5, the condition for partial interdigitation is that the absolute chain-length asymmetry has a value less than approximately: $|\Delta n + \Delta n_o| < 0.45n$ (where Δn_o is the intrinsic asymmetry between the *sn*-1 and *sn*-2 chains), i.e., is somewhat less than half the mean chain length (cf. [44,45]). For phosphatidylcholines, the innate asymmetry Δn_o arises from the sc/γ configuration of the lipid molecule, with the glycerol backbone oriented preferentially parallel to the bilayer normal and the *sn*-2 chain bent at the C-2 position to achieve parallel packing with the *sn*-1 chain [46,47]. Other glycerol backbone configurations (sc/β, -sc/γ and -sc/β) that are found in the crystal structures of different phospholipid species will give rise to different values of Δn_o, if they occur also in the hydrated bilayer state.

For the interdigitated sections of the chains, the incremental transition enthalpy and entropy are reduced by amounts Δh and Δs, respectively, relative to those (ΔH_{inc} and ΔS_{inc}) for the sections of the chain with full intramolecular overlap, i.e., have the values ($\Delta H_{inc} - \Delta h$) and ($\Delta S_{inc} - \Delta s$), respectively. The dependences of the transition enthalpy and transition entropy on both mean chain length and chain asymmetry are then given by [14]:

$$\Delta H_m(n, \Delta n) = \Delta H_{inc}(n - n_H - h' |\Delta n + \Delta n_o|) \quad (6)$$

$$\Delta S_m(n, \Delta n) = \Delta S_{inc}(n - n_S - s' |\Delta n + \Delta n_o|) \quad (7)$$

where n_H and n_S are now the end contributions that are not included in the chain asymmetry, which is given explicitly here by the final terms on the right of Eqs. 6 and 7. The reduced quantities $h' = \Delta h/\Delta H_{inc}$ and $s' = \Delta s/\Delta S_{inc}$ are the fractional deficits in the incremental transition enthalpy and entropy, respectively, for those sections of the chain that do not have intramolecular overlap (see Fig. 2). They are normalized with the corresponding full incremental values for chains with intramolecular overlap, and both are dimensionless.

From Eqs. (2), (6) and (7), the chain-length dependence of the chain-melting temperature, when the asymmetry in chain length, Δn, is considered explicitly, is given by:

$$T_m(n, \Delta n) = T_m^\infty \left(\frac{n - n_H - h' |\Delta n + \Delta n^o|}{n - n_S - s' |\Delta n + \Delta n^o|} \right) \quad (8)$$

Eq. (8) is able to describe the dependence of the chain-melting temperature, T_m, on chain asymmetry for lipids of fixed mean chain length, over the range of asymmetries that corresponds to the partially interdigitated gel state (see Fig. 3). Also the dependence on mean chain length for fixed asymmetry, and on the length of one chain with that of the other fixed, is well described by this equation ([14], and see Figs. 4 and 7 given later).

Sphingomyelin is a phosphocholine-containing sphingolipid in which an *N*-acyl chain is amide-linked to sphingosine (sphing-4-enine). The long-chain base has a fixed length of 18 C atoms, but the length of the *N*-acyl chain is variable and can exceed that of sphingosine by a considerable amount in natural sphingolipids. The glycerolipid analogue of sphingomyelin is phosphatidylcholine with *sn*-1 chain of fixed length and variable-length *sn*-2 chain. Fig. 4 (solid squares) shows the dependence of the chain-melting transition temperature of sphingomyelins on length, n_2, of the *N*-acyl chain, for

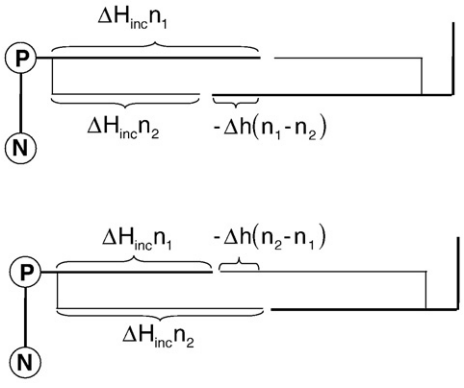

Fig. 2. Schematic diagram of the chain packing of phosphatidylcholines with *sn*-1 and *sn*-2 chains of unequal length (n_1 and n_2, respectively) in a partially interdigitated gel phase. The incremental chain-melting transition enthalpies (per CH_2 group) are ΔH_{inc} for *sn*-1 and *sn*-2 chains overlapping in the same diacyl lipid molecule, and those from the chains overlapping from opposed molecules are $\Delta H_{inc} - \Delta h$. Similar considerations apply to the incremental chain-melting entropies.

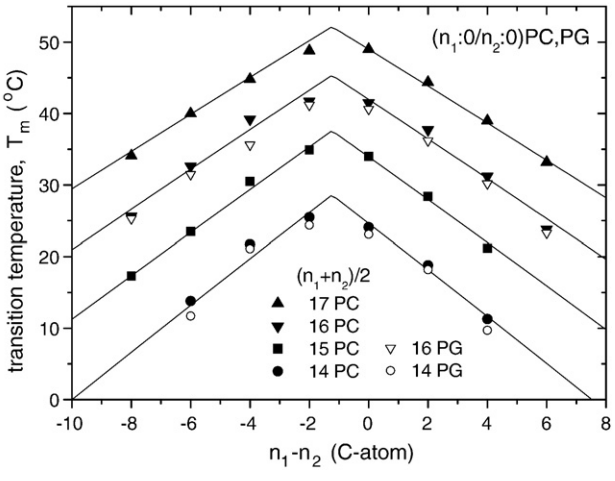

Fig. 3. Dependence of the chain-melting transition temperature of asymmetric phosphatidylcholines (solid symbols, PC, [44,45,48]) and phosphatidylglycerols (open symbols, PG, [49]) on the difference in length, $\Delta n = n_1 - n_2$, between the *sn*-1 and *sn*-2 chains. Data are given for different mean chain lengths which are maintained fixed at $n = (n_1 + n_2)/2 = 17$, 16, 15 or 14, as indicated, and moderate chain asymmetries that correspond to formation of partially interdigitated gel phases. Solid lines are non-linear, least-squares fits of Eq. (8) to the data for PC. Fitting parameters are given in Table 2.

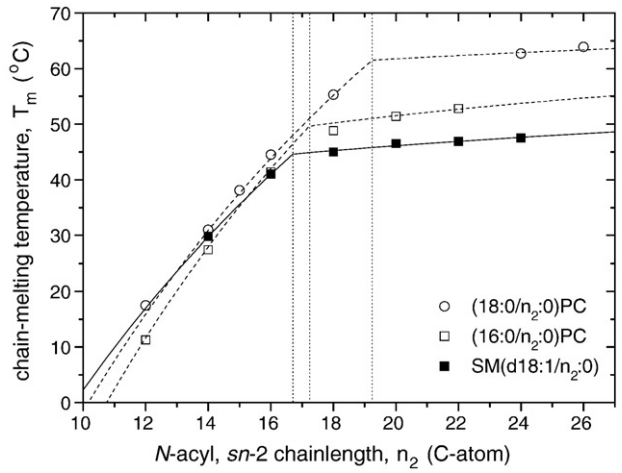

Fig. 4. Dependence of the chain-melting transition temperature of sphingomyelins with fixed sphingoid chain (solid squares; [50]) and asymmetric phosphatidylcholines (open symbols) of fixed *sn*-1 chain length ($n_1 = 16$, 18) that form partially interdigitated gel phases [18,51], on length, n_2, of the *N*-acyl or *sn*-2 chain, respectively. Solid and dashed lines are predictions of Eq. (8) for partially interdigitated gel phases using the parameters given in Table 2. Vertical dotted lines indicate the position for matching of the effective lengths of *N*-acyl and sphingosine chains or *sn*-1 and *sn*-2 chains.

a fixed sphingoid chain. The chain-melting temperature does not vary greatly with increasing *N*-acyl chain length for chains longer than 18 C-atoms (equal to that of sphingosine), but decreases abruptly for shorter chains. Comparison with phosphatidylcholine bilayers shows that this behaviour is characteristic of chain asymmetry, which causes partially interdigitated gel phases to form. Open symbols given in Fig. 4 show the dependence of the chain-melting temperature of phosphatidylcholines on the length, n_2, of the *sn*-2 chain, for a fixed *sn*-1 chain length of $n_1 = 16$ or 18 C-atoms (i.e., comparable to that of sphingosine). The dotted lines in Fig. 4 are predictions of Eq. (8) with the parameters of Table 2 for asymmetric phosphatidylcholines that form partially interdigitated gel phases. A strong similarity with the dependence on *N*-acyl chain length for sphingomyelins is seen clearly. The point at which the transition temperature decreases abruptly corresponds to matching of the effective lengths for the *sn*-1 and *sn*-2 chains, i.e., $n_2 = n_1 + \Delta n_o = 17.24$ and 18.24 for the two phosphatidylcholine series. For the sphingomyelin series, on the other hand, this matching point occurs at a lower value, $n_2 \approx 16.7$, than for phosphatidylcholine with $n_1 = 18$ because the *N*-acyl chain is attached at the 2-position of the 18-carbon sphingosine chain. The corollary of this is that the *N*-acyl chain in sphingomyelin has a bent conformation at the point of attachment that is similar to that of the *sn*-2 chain in phosphoglycerolipids.

The data set for sphingomyelins is insufficient to parameterise Eq. (8) uniquely. However, it can describe the dependence of chain-melting on *N*-acyl chain length with good precision. The solid line in Fig. 4 represents a least squares optimisation with the fractional deficits in incremental transition enthalpy and entropy constrained equal to the values found for phosphatidylcholine. Even so, the entropic end contribution is not determined with any degree of precision. Therefore, this value was also fixed, at $s' = 0$, providing an equally good fit, which is that given in Fig. 4. Nevertheless, as discussed above, the value of the offset, Δn_o, between the sphingosine and *N*-acyl chains is reasonably well defined in this procedure.

Table 2 summarises non-linear, least-squares fitting parameters of Eq. (8), for phosphatidylcholines, phosphatidylglycerols and phosphatidylethanolamines with mean chain lengths in the range $14 \le n \le 18$ and asymmetries in the range $-8 \le \Delta n \le 6$, depending on chain length, and for the more restricted data with sphingomyelin. The values of T_m^∞ lie in much the same range as found for lipids with symmetric chains in Table 1. This is as expected, because T_m^∞ corresponds to the chain-melting temperature extrapolated to chain lengths at which the contribution from fully overlapping chains dominates over all others. For the glycerolipids, the values of Δn_o are in the range expected (~1.5 CH_2 units) from the inherent conformational asymmetry in attachment of the *sn*-1 and *sn*-2 chains to the glycerol backbone that arises from the sc/γ configuration [57–59], and which appears also to be preserved in sphingomyelins. The values of n_H and n_S in Table 2 differ from those for the same lipid species, but with symmetrical chains, that are given in Table 1 because, in the latter case, they contain end contributions from the innate asymmetry between the *sn*-1 and *sn*-2 chains that is allowed for explicitly (by the Δn_o term) in Table 2. Nonetheless, the characteristic differences between the species with different polar head groups are preserved.

5. Chain asymmetry—full interdigitation

For larger asymmetries in chain length between the *sn*-1 and *sn*-2 chains, the longer chain interdigitates fully between those of the apposing bilayer leaflet (see Fig. 5). As seen below, the condition for formation of this mixed interdigitated gel phase is that the absolute chain-length asymmetry has a value greater than approximately: $|\Delta n + \Delta n_o| > 0.45n$, i.e., approaching half the mean chain length (cf. refs. [44,45]). As seen from Fig. 4, to within end effects, fully matched interdigitation is achieved in the mixed interdigitated phase when one chain is twice as long as the other: $n_1 = 2n_2$, or vice-versa. This corresponds to an absolute lipid chain-length asymmetry of $|\Delta n + \Delta n_o| = {}^2/_3 n$ for nearly exact matching.

Chain-melting transition temperatures, enthalpies and entropies initially increase with increasing lipid chain-length asymmetry for mixed interdigitated bilayers. This reverses the trend found for lipid bilayers with partially interdigitated gel phases. On further increasing the chain-length asymmetry in the mixed interdigitated phase, transition temperatures, enthalpies and entropies reach a maximum for fully matched interdigitated chains, and then subsequently decrease (see Fig. 6). The dependences of the chain-melting enthalpy and entropy on absolute chain-length asymmetry, $|\Delta n + \Delta n_o|$, and

Table 2
Dependence of chain-melting temperature on chain-length asymmetry ($-8 \le \Delta n \le 6$), according to Eq. (8), for mixed-chain phosphatidylcholines (n_1:0/n_2:0)PC, phosphatidylethanolamines (n_1:0/n_2:0)PE, phosphatidylglycerols (n_1:0/n_2:0)PG and sphingomyelins SM(d18:1/n_2:0) that form partially interdigitated gel phases (see ref. [14]).

Lipid	T_m^∞ (K)	n_H	n_S	Δn_o	h'	s'
PC[a]	426.4	4.88 ± 0.34	1.12 ± 0.47	1.24 ± 0.05	0.117 ± 0.078	0.03 ± 0.11
PE[b]	432 ± 17	3.3 ± 2.2	−0.2 ± 3.4	1.20 ± 0.20	0.34 ± 0.15	0.33 ± 0.20
PG[c]	373.2 ± 11.4	8.06 ± 0.63	6.64 ± 1.00	1.27 ± 0.10	0.11 ± 0.10	0.06 ± 0.13
SM[d]	413.5 ± 2.6	4.02 ± 0.09	0[e]	−1.29 ± 0.10	0.117[e]	0.0287[e]

[a] Experimental data fitted are from refs. [44,45,48,52]. The fitting parameters are identical to those given in ref. [14], although previously the data set for $(n_1 + n_2)/2 = 16$ was omitted from the fit.
[b] Experimental data fitted are from refs. [21,22,53–56].
[c] In 0.15 M NaCl, 50 mM Hepes, 1 mM EDTA (pH 7.4). Experimental data fitted are from refs. [23,49].
[d] Experimental data fitted are from ref. [50].
[e] Maintained fixed.

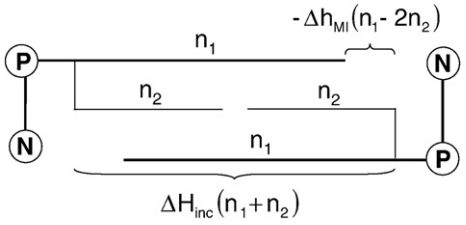

Fig. 5. Schematic diagram of the chain packing of phosphatidylcholines with *sn*-1 and *sn*-2 chains of unequal length (n_1 and n_2, respectively) in a mixed interdigitated gel phase. The longer chain (here *sn*-1) is approximately twice the length of the shorter chain. The incremental chain-melting transition enthalpies (per CH_2 group) are ΔH_{inc} for overlapping *sn*-1 and *sn*-2 chains, and $\Delta H_{inc}-\Delta h_{MI}$ for non-overlapped chain segments. Similar considerations apply to the incremental chain-melting entropies.

mean chain length, n, for lipids that form mixed interdigitated gel phases can be described by:

$$\Delta H_m(n,\Delta n) = \Delta H_{inc}(n - n_H) - \Delta h_{MI}\,|\,|\Delta n + \Delta n_o| - {}^2/_3 n + \Delta n_{MI}\,| \quad (9)$$

$$\Delta S_m(n,\Delta n) = \Delta S_{inc}(n - n_S) - \Delta s_{MI}\,|\,|\Delta n + \Delta n_o| - {}^2/_3 n + \Delta n_{MI}\,| \quad (10)$$

where Δh_{MI} and Δs_{MI} are the deficits in incremental enthalpy and entropy, respectively, for non-overlapped chain segments (see Fig. 5), n_H and n_S now include all end contributions not specifically involving non-overlapped chain segments, and Δn_{MI} represents the offset of fully matching interdigitation from the asymmetry defined by $|\Delta n + \Delta n_o| = {}^2/_3 n$. If exact matching of the overlapped chains in the mixed interdigitated phase were achieved with one chain twice the length of the other, then Δn_{MI} would be zero. The incremental transition enthalpy and transition entropy for chain segments that are not overlapped are given by $\Delta H_{inc}-\Delta h_{MI}$ and $\Delta S_{inc}-\Delta s_{MI}$, respectively, irrespective of which chain is the longer. This equality of slopes (Δh_{MI} and Δs_{MI}) on either side of the maximum (for constant mean chain length) is a simplifying assumption, because this corresponds to non-overlap of chains on the low-asymmetry side, but to overlap with the headgroups on the high-asymmetry side (see Fig. 5). However, the current data (cf. Fig. 6) do not justify a more elaborate model.

From Eqs. (2), (9) and (10), the dependence of the chain-melting temperature on absolute chain-length asymmetry and mean chain length for lipids that form the mixed interdigitated gel phase is given by:

$$T_m(n,\Delta n) = T_m^{\infty}\left(\frac{n - n_H - h'_{MI}\,|\,|\Delta n + \Delta n_o| - {}^2/_3 n + \Delta n_{MI}\,|}{n - n_S - s'_{MI}\,|\,|\Delta n + \Delta n_o| - {}^2/_3 n + \Delta n_{MI}\,|}\right) \quad (11)$$

where h'_{MI} ($=\Delta h_{MI}/\Delta H_{inc}$) and s'_{MI} ($=\Delta s_{MI}/\Delta S_{inc}$) are the fractional deficits in incremental enthalpy and entropy, respectively, for non-overlapped chain segments. Again these quantities are normalized with the corresponding full incremental values (ΔH_{inc} and ΔS_{inc}) for chains with intramolecular overlap, and both are dimensionless.

Equation 11 is able to describe the dependence of the chain-melting temperature, T_m, on chain asymmetry reasonably well for lipids of fixed mean chain length, over the range of asymmetries that corresponds to the mixed interdigitated gel state (see Fig. 6). Table 3 summarises non-linear, least-squares fitting parameters of Eq. (11), for phosphatidylcholines with mean chain lengths in the range $14 \le n \le 17$ and asymmetries in the ranges $\Delta n \le -8$ and $\Delta n \ge 6$, depending on chain length. The value of T_m^{∞} lies in the usual range for fully overlapped chains (cf. Tables 1 and 2), but unfortunately n_H and n_S cannot be determined independently with any degree of accuracy. Therefore, a fixed value of $n_S = 0$ was used in the fitting, which means that physical significance cannot be attributed to these values (nor to h'_{MI} and s'_{MI}). However, it is significant that the value of Δn_{MI} remains consistently small, confirming that fully matched interdigitation is achieved with one chain almost exactly twice the length of the other.

The abrupt discontinuity between the predictions of Eqs. (8) and (11) for the dependence of chain-melting temperature on chain asymmetry that is seen in Fig. 6 (dotted and solid lines, respectively) defines the boundary between the partially and mixed interdigitated regimes. The ratio of absolute asymmetry to mean chain length, $|\Delta n + \Delta n_o|/n$, at the cross-over point varies between 0.44 and 0.46 with decreasing mean chain length. Strictly speaking, comparison should be made with the longer of the two chain lengths [44,45], but it seems that using the mean chain length also provides a reasonably reliable indicator.

Fig. 7 shows the dependence of chain-melting temperature on length of the *sn*-1 chain for lipids with fixed chain asymmetries. Eq. (11) is able adequately to describe the dependence on mean chain length for the lipid series forming mixed interdigitated gel phases (solid symbols), although not quite so well as Eq. (8) describes that for the series forming partially interdigitated gel phases (open symbols).

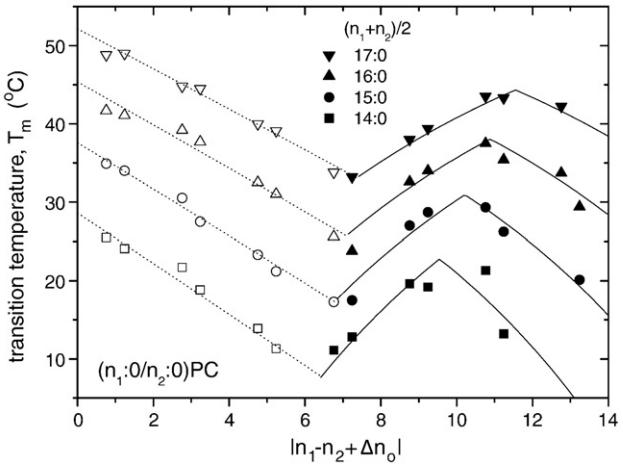

Fig. 6. Dependence of the chain-melting transition temperature of asymmetric phosphatidylcholines with mixed interdigitated gel phases (solid symbols; [45,60,61]), or partially interdigitated gel phases (open symbols; [44,45,48]), on the absolute difference in length, $|\Delta n + \Delta n_o| \equiv |n_1 - n_2 + \Delta n_o|$, between the *sn*-1 and *sn*-2 chains. Data are given for different mean chain lengths which are maintained fixed at $n = (n_1 + n_2)/2 = 17$, 16, 15 or 14, as indicated, and include large asymmetries that correspond to formation of mixed interdigitated gel phases. Solid lines are non-linear, least-squares fits of Eq. (11) to the data for mixed interdigitated gel phases; fitting parameters are given in Table 3. Dotted lines are non-linear, least-squares fits of Eq. (8) to the data for partially interdigitated gel phases (cf. Fig. 3).

6. Unsaturated chains

The chain-melting transition temperatures of diacyl phospholipids with symmetrical *cis*-monoenoic chains, or with a saturated *sn*-1 chain and *cis*-monoenoic *sn*-2 chain, display a biphasic dependence on the position, n_u, of the double bond in the chain [63–65]. For

Table 3
Dependence of chain-melting temperature on absolute chain-length asymmetry, $|\Delta n + \Delta n_o|$, ($\Delta n \le -8$ and $\Delta n \ge 6$) according to Eq. (11) for mixed-chain phosphatidylcholines (n_1:0/n_2:0)PC that form mixed interdigitated gel phases.

Lipid	T_m^{∞} (K)	n_H	n_S	Δn_{MI}	h_{MI}	s_{MI}
PC[a]	418.1 ± 7.6	4.09 ± 0.20	0[b]	−0.21 ± 0.09	0.741 ± 0.313	0.862 ± 0.426

Experimental data fitted are from refs. [45,60,61].
[a] $\Delta n_o = 1.24$ for PC (see Table 2).
[b] Maintained fixed.

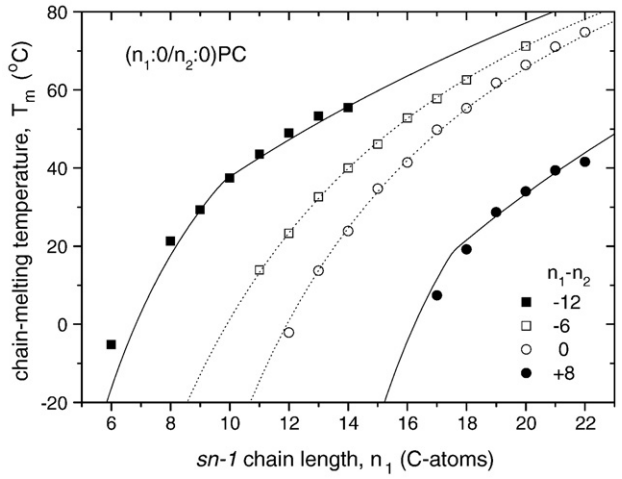

Fig. 7. Dependence of the chain-melting transition temperature of asymmetric phosphatidylcholines with mixed interdigitated gel phases (solid symbols; [45,60–62]), or partially interdigitated gel phases (open symbols; [18,51]), on length, n_1, of the *sn*-1 chain for lipids with fixed chain-length asymmetry, $\Delta n = n_1 - n_2$, as indicated. Solid lines are predictions of Eq. (11) for mixed interdigitated gel phases using the parameters given in Table 3. Dotted lines are corresponding predictions of Eq. (8) for partially interdigitated gel phases.

constant chain length n of the unsaturated chain, the transition temperature reaches a minimum value T_m^∞ for some critical position, $n_u = n_c$, of the double bond that is close to, but not coincident with, the chain midpoint. Fig. 8 shows the dependence of the chain-melting transition temperature, enthalpy and entropy on position of the *cis*-double bond for symmetric monoenoic diacyl phosphatidylcholines with a fixed chain length of 18 C-atoms. The dependence of the calorimetric enthalpy and entropy on double-bond position is not great for chains of fixed length. Nevertheless, a bilinear dependence analogous to that found above is suggested, in which transition enthalpy, ΔH_m, and entropy, ΔS_m, change symmetrically with distance of the double bond from the critical position, n_c [16]:

$$\Delta H_m(n, n_u) = \Delta H_m^c(n) + \Delta h_c |n_u - n_c(n)| \quad (12)$$

$$\Delta S_m(n, n_u) = \Delta S_m^c(n) + \Delta s_c |n_u - n_c(n)| \quad (13)$$

where $\Delta H_m^c(n)$ and $\Delta S_m^c(n)$ are the extremum values of $\Delta H_m(n,n_u)$ and $\Delta S_m(n,n_u)$, respectively, which are obtained with the double bond at the critical position $n_u = n_c(n)$. The quantities that depend on chain length are indicated as implicit functions of n. These equations imply that contributions to the calorimetric quantities differ for the sections of the chain above and below the double bond, depending on which is the longer (see Fig. 10, given later).

From Eqs. (2), (12) and (13), the dependence of chain-melting temperature on double-bond position for a fixed chain length is given by:

$$T_m(n, n_u) = T_m^c(n)\left(\frac{1 + h'_c(n)|n_u - n_c(n)|}{1 + s'_c(n)|n_u - n_c(n)|}\right) \quad (14)$$

where $T_m^c(n)$ $(\equiv \Delta H_m^c(n)/\Delta S_m^c(n))$ is the minimum value of the transition temperature for the critical double bond position $n_u = n_c(n)$, and $h'_m(n)$ $(\equiv \Delta h_c/\Delta H_m^c(n))$ and $s'_c(n)$ $(\equiv \Delta s_c/\Delta S_m^c(n))$ are the normalized incremental positional deficits in the calorimetric quantities, which are dimensionless. This equation can describe the dependence of chain-melting temperature on double-bond position for a wide variety of monoenoic phosphatidylcholines and phosphatidylethanolamines with constant chain length (see Fig. 9). The parameters from nonlinear least-squares fitting are given in Table 4. Because the changes in calorimetric properties are relatively small, the constraint $s'_c = 0$ was used in the fitting procedure [16]. This is especially the case for phosphatidylethanolamines, where the change in chain-melting temperature with double-bond position is considerably smaller than for phosphatidylcholines.

As seen from Fig. 10, the symmetrical linear dependence of ΔH_m arises because the incremental enthalpy of the longer chain section, above or below the double bond, is greater by an amount Δh_c than

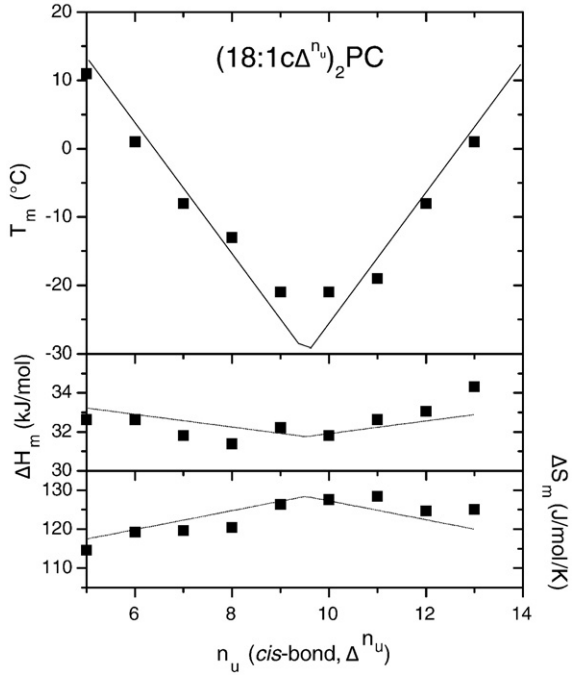

Fig. 8. Dependence of the chain-melting transition temperature, T_m (upper panel) and chain-melting enthalpy, ΔH_m, and entropy, ΔS_m (lower two panels) of symmetric monoenoic phosphatidylcholines with a fixed chain length, $n = 18$, on position, n_u, of the *cis*-double bond. Data points from ref. [63]. Solid lines are least-squares fits of Eqs. (14), (12) and (13) to the data for transition temperature, enthalpy and entropy, respectively.

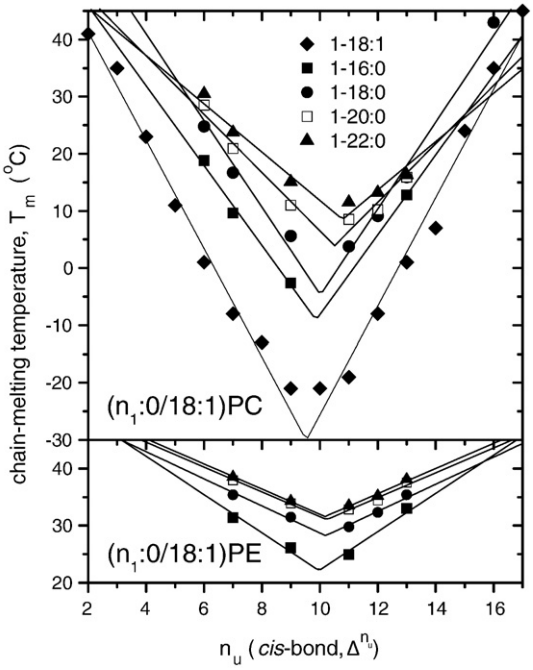

Fig. 9. Dependence of the chain-melting transition temperatures of 1-acyl-2-(18:1cΔ^{n_u})-*sn*-glycero-3-phosphocholines (upper panel) and -phosphoethanolamines (lower panel) with fixed *sn*-1 chain length on position, n_u, of the *cis*-double bond. Data points are from refs. [63–68]. Solid lines are least-squares fits of Eq. (14).

Table 4
Dependence of chain-melting temperature on double-bond position, n_u, according to Eq. (14), for monoenoic phosphatidylcholines (PC) and phosphatidylethanolamines (PE) of constant chain length [16].

Lipid	T_m^c (K)	n_c	h_c'	s_c'
(18:1cΔ^{n_u})$_2$PC	243.1 ± 1.7	9.53 ± 0.09	0.039 ± 0.002	0[a]
(16:0/18:1cΔ^{n_u})PC	264.1 ± 2.4	9.87 ± 0.14	0.026 ± 0.003	0[a]
(18:0/18:1cΔ^{n_u})PC	268.5 ± 1.8	10.02 ± 0.12	0.028 ± 0.002	0[a]
(20:0/18:1cΔ^{n_u})PC	277.1 ± 1.8	10.51 ± 0.19	0.018 ± 0.003	0[a]
(22:0/18:1cΔ^{n_u})PC	281.6 ± 2.0	10.78 ± 0.23	0.015 ± 0.003	0[a]
(20:0/20:1cΔ^{n_u})PC	289.9 ± 1.1	11.57 ± 0.20	0.0145 ± 0.0011	0[a]
(16:0/18:1cΔ^{n_u})PE	295.3 ± 1.6	9.97 ± 0.20	0.011 ± 0.002	0[a]
(18:0/18:1cΔ^{n_u})PE	301.4 ± 0.4	10.20 ± 0.12	0.008 ± 0.001	0[a]
(20:0/18:1cΔ^{n_u})PE	304.2 ± 0.5	10.23 ± 0.11	0.0072 ± 0.0008	0[a]
(22:0/18:1cΔ^{n_u})PE	304.8 ± 0.4	10.18 ± 0.08	0.0072 ± 0.0006	0[a]
(20:0/20:1cΔ^{n_u})PE	314.1 ± 0.6	11.83 ± 0.21	0.0079 ± 0.0060	0[a]

Experimental data fitted are from refs. [63–68]. Data sets used and fitting parameters are those given in ref. [16].
[a] Maintained fixed.

that of the shorter section. The incremental transition enthalpy and transition entropy are ΔH_{inc} and ΔS_{inc}, respectively, for the longer chain section, and $\Delta H_{inc} - \Delta h_c$ and $\Delta S_{inc} - \Delta s_c$, respectively, for the shorter chain section on the other side of the double bond. The molecular origin for this difference is most probably that, in the gel phase, the perturbation introduced by the double bond causes less optimal packing of the shorter section of the chain than of the longer, because it is energetically more favourable for the longer section to pack well. Note that the values of h_c' that are given in Table 4 are all positive.

Because of "end" effects, the critical position of the double bond, n_c, in Eqs. 12 and 13 is offset from the centre of the chain, $n/2$, by an amount $\delta n_c \equiv (\delta n_u - \delta n)/2 \sim 0.9-1.8$ [16]:

$$n_c(n) = n/2 + (\delta n_u - \delta n)/2 \tag{15}$$

where δn_u and δn (multiplied by the corresponding incremental quantities) represent the constant end contributions to the transition enthalpy (and entropy) for the upper and lower sections, respectively, of the unsaturated chain. From Table 4, for lipids in which the length of the unsaturated chain is held constant at 18 C-atoms, the offset from the middle of the chain is in the range: $\delta n_c \sim 0.9-1.8$ for the (n_1:0/18:1cΔ^{n_u})PC series. End contributions to the upper and lower

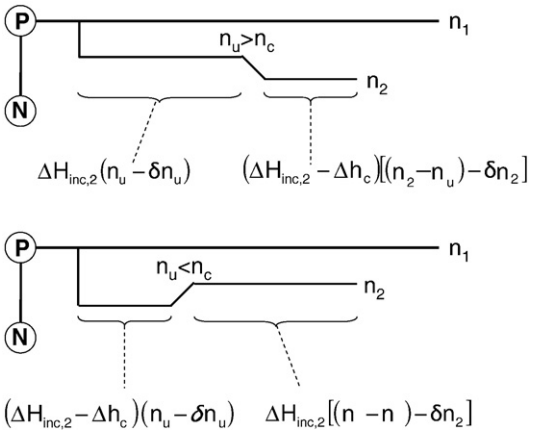

Fig. 10. Schematic diagram of the chain packing in phospholipids with monoenoic *sn*-2 chains (n_2:1cΔ^{n_u}). The incremental chain-melting enthalpies are ΔH_{inc} and $\Delta H_{inc} - \Delta h_c$ per CH_2 group for the longer and shorter segments, respectively, of the *sn*-2 chain. The effective length of the upper chain segment is $n_u - \delta n_u$ and that of the lower segment is $(n_2 - n_u) - \delta n_2$. Equivalent considerations hold for symmetrical monoenoic diacyl phospholipids in which the *sn*-1 chain is also unsaturated, and the effective length of the lower chain segments is then both $(n - n_u) - \delta n$. Similar considerations apply to the incremental chain-melting entropies.

sections of the chain arise from the $g^+s^+\Delta s^+$ configuration about the *cis*-double bond, which optimizes packing of the unsaturated chains in the gel phase, and from the bent configuration at the C-2 position of the *sn*-2 chain. From molecular mechanics calculations, Huang and co-workers [69] conclude that $\delta n_u = 5$ and $\delta n_2 = 2$, which results in a predicted offset of $\delta n_c = 1.5$, hence substantiating the connection of the thermodynamic model with lipid chain structure.

For lipids with an unsaturated *sn*-2 chain of fixed length, the dependence of the extremum value, $\Delta H_m^c(n_1)$, in Eq. (12) on length, n_1, of the saturated *sn*-1 acyl chain is given by an expression analogous to Eq. (3):

$$\Delta H_m^c(n_1) = \Delta H'_{inc,1}\left(n_1 - n_{1,H}\right) \tag{16}$$

where $\Delta H'_{inc,1}$ is the incremental transition entropy per CH_2 group of the *sn*-1 chain, and $n_{1,H}$ represents not only end effects but all contributions that do not depend on n_1, including those from the *sn*-2 chain. An equivalent expression holds for the dependence on n_1 of the extremum value $\Delta S_m^c(n_1)$ in Eq. (13). As regards chain-length asymmetry, the *sn*-2 chain is assumed shorter than the *sn*-1 chain (after allowing for the shortening effects of the double bond and the bent conformation at the glycerol backbone). This holds for all the lipids that are included in Table 4. Thus from Eqs. (2), (16) and the equivalent for $\Delta S_m^c(n_1)$, the dependence of the minimum transition temperature, $T_m^c(n_1)$, on length of the *sn*-1 chain can be expressed in a form analogous to Eq. (5):

$$T_m^c(n_1) = T_m^{c,\infty}\left(1 - \frac{n_{1,H} - n_{1,S}}{n_1 - n_{1,S}}\right) \tag{17}$$

where $T_m^{c,\infty}$ ($\equiv \Delta H'_{inc,1}/\Delta S'_{inc,1}$) is the value of the minimum transition temperature, $T_m^c(n_1)$, extrapolated to infinite *sn*-1 chain length. The parameters $n_{1,H}$ and $n_{1,S}$ are the *sn*-1 chain lengths at which the extremum values of the transition enthalpy ($\Delta H_m^c(n_1)$) and transition entropy ($\Delta S_m^c(n_1)$), respectively–which are obtained with the critical double-bond position $n_u = n_c(n_2)$–extrapolate to zero.

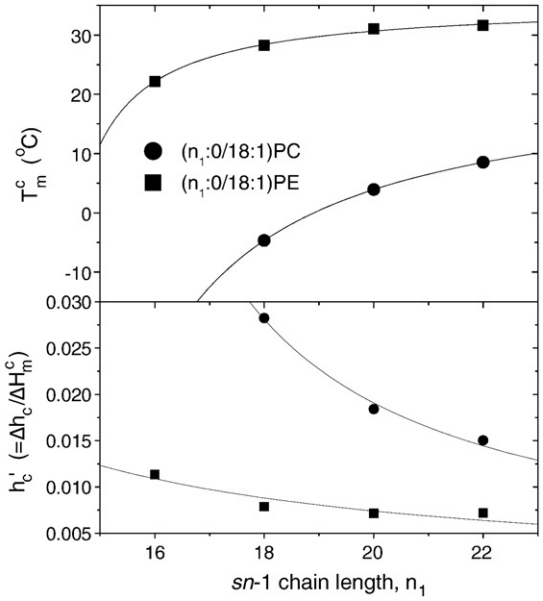

Fig. 11. Dependence on length, n_1, of the saturated *sn*-1 acyl chain of the chain-melting temperature minimum $T_m^c(n_1)$ (upper panel), and incremental positional enthalpic deficit $h_c'(n_1)$ (lower panel), for 1-(n_1:0)-2-(n_2:1cΔ^{n_u}) phosphatidylcholines (circles) and phosphatidylethanolamines (squares). Solid lines are non-linear least-squares fits of Eqs. 17 and 18 for $T_m^c(n_1)$ and $h_c'(n_1)$, respectively [16].

Fig. 11 (top panel) gives the dependence of the transition-temperature minimum on length of the *sn*-1 chain for both (n_1:0/18:1cΔ^{n_u})PC and PE series with unsaturated *sn*-2 chains. Equation 17 is able to describe the dependence on n_1 with high precision. The fitting parameters are given in Table 5. They differ greatly from those for saturated symmetrical diacyl PCs and PEs, which are given in Table 1, because of the presence of the *cis*-double bond in the *sn*-2 chain, and because the length of the latter is held constant at 18 C-atoms. Interestingly, the values of $n_{1,H}$ and $n_{1,S}$ are rather similar for the phosphatidylcholine and phosphatidylethanolamine series. This suggests that, for the double bond at the critical chain position, the effects of unsaturation tend to outweigh the differences between headgroups, most probably leading to greater headgroup hydration than is found for saturated phosphatidylethanolamines. Nonetheless, the origin of the dependence of the transition temperature of lipids with unsaturation in the biologically relevant *sn*-2 chain, on length of the saturated chain in the *sn*-1 position (also biologically relevant), is exactly the same as that already characterized for the symmetrical disaturated phospholipids. Note that when the *sn*-1 chain of phosphatidylcholine is also unsaturated (18:1cΔ^{n_u}), the minimum transition temperature is lower than that for any of the analogues with saturated *sn*-1 chain. Also, for the same saturated *sn*-1 chain (20:0), the minimum transition temperature increases on increasing the chain length of the *sn*-2 chain from (18:1Δ^{n_u}) to (20:1Δ^{n_u}).

The incremental positional enthalpic deficit, h'_c, also depends on length, n_1, of the *sn*-1 chain, because of the normalisation by $\Delta H^c_m(n_1)$: $h'_c(n) \equiv \Delta h_c / \Delta H^c_m(n)$. From Eq. (16), the dependence on n_1 is therefore given by:

$$h'_c(n_1) = \frac{\Delta h_c / \Delta H'_{inc,1}}{n_1 - n_{1,H}} \tag{18}$$

The bottom panel of Fig. 11 shows that Eq. (18) can describe the dependence on *sn*-1 chain length for both the phosphatidylcholine and phosphatidylethanolamine series quite well. The fitting parameters, $\Delta h_c/\Delta H'_{inc,1}$ and $n_{1,H}$, are given in Table 5. The value of the latter is consistent with that obtained from fits of the transition temperature $T^c_m(n_1)$ for phosphatidylcholine; for phosphatidylethanolamines the chain-length dependence is rather weak and therefore $n_{1,H}$ is not determined very accurately. The significant result is that the dependence on position of the double bond in the *sn*-2 chain is well determined by the model indicated in Fig. 10, with a constant value for the enthalpic deficit Δh_c, independent of the *sn*-1 chain length.

7. Methyl-branched chains

Chains with methyl branches are used by micro-organisms, as a chemically more stable alternative to *cis*-double bonds, for reducing the chain-melting temperature of the membrane lipids. An extreme example is the phytanyl chain of archaeal lipids which contains four branched methyl groups in a chain of 16 C-atoms.

As for a *cis*-double bond, a single branched methyl group divides the lipid chain into a longer and a shorter section, resulting in a biphasic dependence of chain-melting temperature on position of methyl substitution, with a minimum at a characteristic position $n_{Me} = n_c$ (see Fig. 12). Unlike the situation with *cis*-double bonds, the chain-melting enthalpy and entropy also depend very strongly on position, n_{Me}, of methyl substitution in the chain. The straight lines in Fig. 12) correspond to bilinear fits of the transition enthalpy and entropy, according to Eqs. (12) and (13) with $n_{Me} \equiv n_u$. The dependence of the chain-melting temperature on methyl position can be described by Eq. (14) with parameters T^c_m, n_c, h_c' and s_c', in exactly the same way as for unsaturated chains.

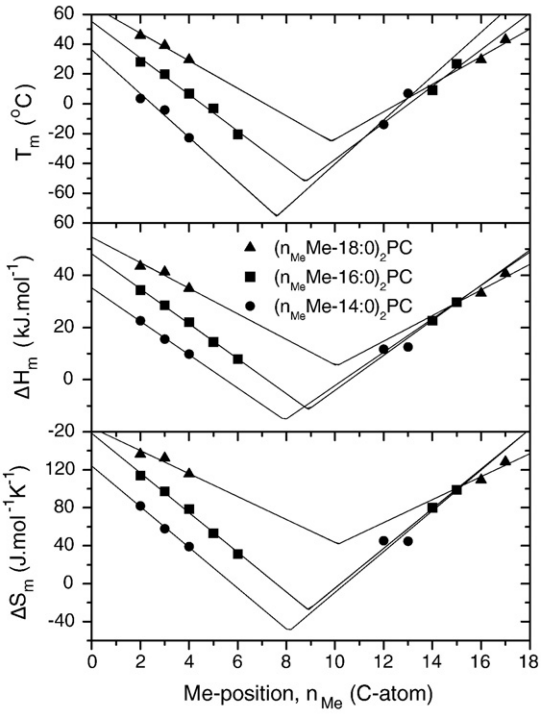

Fig. 12. Dependence of the chain-melting transition temperature, T_m (upper panel) and chain-melting enthalpy, ΔH_m, and entropy, ΔS_m (lower two panels) of symmetric methyl-branched diacyl phosphatidylcholines with fixed chain lengths of $n = 14$ (circles), 16 (squares) or 18 (triangles), on position, n_{Me}, of methyl substitution. Data points from refs. [26,28 and 29]. Solid lines are least-squares fits of Eqs. (14), (12) and (13) to the data for transition temperature, enthalpy and entropy, respectively.

Parameters from non-linear least-squares fits are given in Table 6. The (interpolated) values for the critical chain position, n_c, of the methyl group indicate that the maximum depression in chain-melting transition is obtained for a methyl group located at the centre of the chain: $n_{Me} \approx n/2$. The values of the minimum transition temperature, T^c_m, for C-18 chains indicate that a methyl group is equally effective as a *cis*-double bond in lowering the chain-melting transition.

8. α-Branched chains and chain-modified headgroups

Addition of a third chain, either attached to the lipid headgroup (as in *N*-acyl phosphatidylethanolamines) or as a branch of one of the glycerol-attached chains (as in α-branched mycolic acids, or in lipid A of lipopolysaccharides), gives further contributions to the thermodynamics of chain-melting (see Fig. 13). As for mismatch in chain length of the two glycerol-attached chains, the chain-melting temperature

Table 5
Dependence of transition temperature minimum, T^c_m, and incremental positional enthalpic deficit, h'_c, from Table 4 on *sn*-1 chain length, n_1, according to Eqs. (17) and (18), respectively, for *sn*-2 monoenoic phosphatidylcholines (PC) and phosphatidylethanolamines (PE) [16].

Lipid	$T_m^{c,\infty}$ (K)	$n_{1,H}$-$n_{1,S}$	$n_{1,S}$	$\Delta h_c/\Delta H'_{inc,1}$	$n_{1,H}$
(n_1:0/18:1)PC	298.6	0.438	13.41	0.119 ± 0.013	13.8 ± 0.5
(n_1:0/18:1)PE	308.6 ± 1.7	0.10 ± 0.05	13.7 ± 0.8	0.093 ± 0.028	7.5 ± 3.0

Note: fitting parameters are those given in ref. [16].

Table 6
Dependence of chain-melting temperature on methyl group position, n_{Me}, according to Eq. (14), for methyl-branched phosphatidylcholines (PC) of constant chain length.

Lipid	T_m^c (K)	n_c	h_c'	s_c'
(n_{Me}Me-14:0)$_2$PC	197.7 ± 14.2	7.60 ± 0.15	0.074 ± 0.020	0[a]
(n_{Me}Me-16:0)$_2$PC	220.9 ± 5.1	8.77 ± 0.11	0.056 ± 0.005	0[a]
(n_{Me}Me-18:0)$_2$PC	248.0 ± 11.1	9.85 ± 0.13	0.037 ± 0.008	0[a]

Experimental data fitted are from refs. [26,28 and 29].
[a] Maintained fixed.

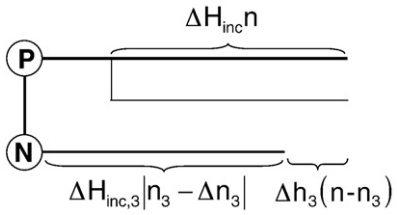

Fig. 13. Schematic diagram of the chain packing in *N*-acyl phosphatidylethanolamines. The incremental chain-melting enthalpy (per CH_2 group) for the *N*-acyl chain is $\Delta H_{inc,3}$ in the regions where the chains overlap, and Δh_3 is an incremental deficit from those regions of the glycerol-attached chains where the *N*-acyl chains do not overlap (see ref. [38]). The sign associated with $\Delta H_{inc,3}$ changes depending on whether the *N*-acyl chain is longer or shorter than the critical length Δn_3, as reflected by the switching function $|n_3\text{-}\Delta n_3|$ (see ref. [15]). The net incremental transition enthalpy with respect to length of the *N*-acyl chain is $(\Delta H_{inc,3} - \Delta h_3)$ for long *N*-acyl chains ($n_3 > \Delta n_3$), and $-(\Delta H_{inc,3} + \Delta h_3)$ for short *N*-acyl chains ($n_3 < \Delta n_3$). (Note that the switching function involving the critical chain length Δn_3 could instead have been applied equivalently to the incremental deficit term Δh_3.)

displays a biphasic dependence on length, n_3, of the third chain. This indicates that, for third chains shorter than a critical length, Δn_3, the packing of the third chain changes from parallel alignment with the *sn*-1 and *sn*-2 chains (cf. [70]) to a less ordered packing mode.

A change in packing mode of the third chain will affect all thermodynamic parameters of the chain-melting transition, as indicated for the enthalpy in Fig. 13. Based on the latter, a biphasic linear dependence on n_3 is assumed for both the transition enthalpy and transition entropy, when the length, *n*, of the glycerol-attached chains is kept fixed [15]:

$$\Delta H_m(n, n_3) = \Delta H_{inc,3}\Big(|n_3 - \Delta n_3| + n_{3,H}(n)\Big) - \Delta h_3 n_3 \quad (19)$$

$$\Delta S_m(n, n_3) = \Delta S_{inc,3}\Big(|n_3 - \Delta n_3| + n_{3,S}(n)\Big) - \Delta s_3 n_3 \quad (20)$$

where $\Delta H_{inc,3}$, $\Delta S_{inc,3}$ are the incremental transition enthalpy and entropy, respectively, for the third chain, and $n_{3,H}(n)$ and $n_{3,S}(n)$ represent all further contributions that are not dependent on the length of the third chain. (For compactness, the term $\Delta h_3 n$ in Fig. 13 is subsumed in the total *n*-dependent term $n_{3,H}(n)$ in Eq. (19), and correspondingly in Eq. (20)). In the absence of the third chain, note that the transition enthalpy and entropy corresponding to the entire lipid molecule are notionally: $\Delta H_m(n) = (n_{3,H}(n) + |\Delta n_3|)\Delta H_{inc,3}$ and $\Delta S_m(n) = (n_{3,S}(n) + |\Delta n_3|)\Delta S_{inc,3}$, respectively. The net incremental transition enthalpy for long third chains ($n_3 > \Delta n_3$) is $(\Delta H_{inc,3} - \Delta h_3)$, and that for short third chains ($n_3 < \Delta n_3$) is $-(\Delta H_{inc,3} + \Delta h_3)$, i.e., is of different magnitude and opposite in sign. This latter feature is the real basis of the thermodynamic model, which is consequently far more general than the specific scheme given in Fig. 13. Similar considerations to those for the transition enthalpy hold also for the transition entropy.

From Eqs. (2), (19) and (20), the dependence of the chain-melting transition temperature on length of the third chain is given by:

$$T_m(n, n_3) = T_m^{(3)} \cdot \left(\frac{|n_3 - \Delta n_3| - h'_3 n_3 + n_{3,H}(n)}{|n_3 - \Delta n_3| - s'_3 n_3 + n_{3,S}(n)} \right) \quad (21)$$

where the parameters $T_m^{(3)}$ ($= \Delta H_{inc,3}/\Delta S_{inc,3}$) and h'_3 ($= \Delta h_3/\Delta H_{inc,3}$), s'_3 ($= \Delta s_3/\Delta S_{inc,3}$) are related directly to the dependence of the calorimetric enthalpy and entropy on length of the third chain. Note that the fractional deficits h'_3 and s'_3 are again dimensionless, but $T_m^{(3)}$ is not the minimum chain-melting temperature, which is given by $T_m(n,\Delta n_3) = T_m^{(3)}(n_{3,H}(n) - h'_3\Delta n_3)/(n_{3,S}(n) - s'_3\Delta n_3)$. A more general treatment that explicitly includes the dependence on length, *n*, of the glycerol-attached chains is given in ref. [15].

Fig. 14 shows the dependence of the chain-melting temperature on length of the third chain for phosphatidylcholines with α-branched *sn*-1 chains, and for *N*-acyl phosphatidylethanolamines and *O*-alkyl phosphatidic acids with headgroup-attached chains. It is seen that Eq. (21) is capable of describing the dependence on length of the third chain, over a wide range that encompasses both the long and short chain-length regimes. Fitting parameters obtained by non-linear, least-squares optimization are given in Table 7. Non-zero values of h'_3 and s'_3 (i.e., of Δh_3 and Δs_3) are required to describe the marked asymmetry in the dependence of chain-melting temperature on length of the third chain that is seen for all lipid systems shown in Fig. 14. Short chains with $n_3 < \Delta n_3$ make a relatively smaller contribution to the total calorimetric enthalpy and entropy than do long chains with $n_3 > \Delta n_3$, because $\Delta h'_3$ and $\Delta s'_3$ are positive. This means that the short chains pack less well in the bilayer structure than do the long chains, or alternatively do not enter the bilayer at all.

For *N*-acyl phosphatidylethanolamines, it is found by spin-label EPR that long *N*-acyl chains pack parallel to the glycerol-attached chains, within the bilayer interior [70]. For short *N*-acyl chains, it is not known with certainty whether they remain in the headgroup region or simply partially disrupt the packing of the glycerol-attached chains. In the case of phosphatidylcholines with α-branched chains, the latter scenario is far the more likely for the short-chain regime. Structural information is not available for the alkyl phosphatidic acids, but it seems highly likely that the shorter chains are located in the head-group region and are disordered. The longer alkyl chains either may enter the bilayer core and pack parallel to the glycerol-attached chains, or possibly might pack closely with one another in a purely hydrocarbon phase above the lipid headgroups.

With the possible exception of TPE, the critical chain length, Δn_3, for the lipids in Fig. 14 is in the region of 9 C-atoms. For chains shorter than this, entropy of disorder presumably begins to outweigh the enthalpic advantages of van der Waals interactions that accrue from

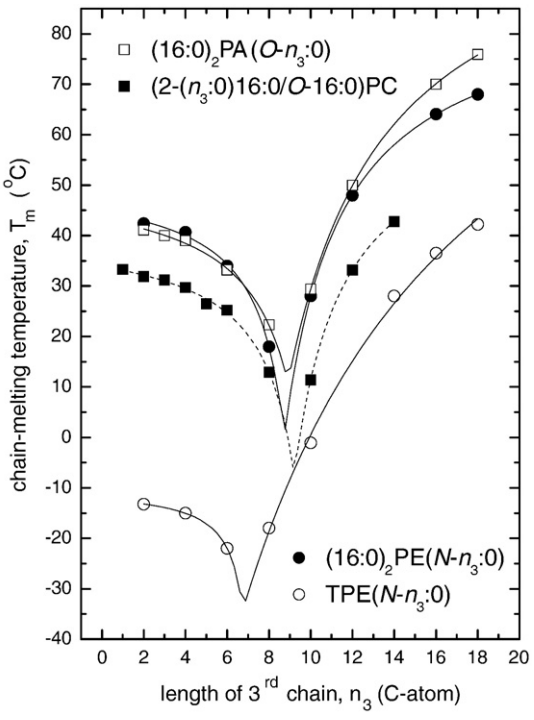

Fig. 14. Dependence of chain-melting transition temperature on length, n_3, of the third lipid chain for 1-(2-alkyl)palmitoyl-2-hexadecyl phosphatidylcholines [■, (2-(n_3:0) 16:0/O-16:0)PC], *N*-acyl dipalmitoyl phosphatidylethanolamines [●, $(16:0)_2$PE(*N*-n_3:0)], *N*-acyl transphosphatidylated phosphatidylethanolamines [○, TPE(*N*-n_3:0)], and *O*-alkyl dipalmitoyl phosphatidic acids [□, $(16:0)_2$PA(*O*-n_3:0)]. Data from refs. [72–76]. Lines are non-linear least squares fits to Eq. (21) [15].

Table 7
Dependence of chain-melting temperatures of α-branched phosphatidylcholines on α-alkyl chain length, n_3, of *N*-acyl phosphatidylethanolamines and *O*-alkyl phosphatidic acids on length, n_3, of the headgroup-attached chains, and of diacyl phosphatidyl-trimethylalkanolamines on the number, n_3, of CH_2 groups between phosphate and headgroup quaternary nitrogen, according to Eq. (21) (see [15]).

Lipid	$T_m^{(3)}$ (K)	h_3'	s_3'	$n_{3,H}$	n l.c.$_{3,S}$	Δn_3
(2-(n_3:0)16:0/*O*-16:0)PC[a]	325.4 ± 2.7	0.13 ± 0.15	0.17 ± 0.15	2.77 ± 1.34	3.49 ± 1.40	9.21 ± 0.11
(*N*-n_3:0)-(16:0)$_2$PE	336.9 ± 3.5	0.28 ± 0.12	0.33 ± 0.12	3.95 ± 0.87	4.71 ± 0.83	8.73 ± 0.09
N-(n_3:0)-TPE[b]	270 ± 43	0.84 ± 0.69	0.89 ± 0.47	6.7 ± 1.4	7.2 ± 3.4	6.7 ± 1.0
(*O*-n_3:0)-(16:0)$_2$PA	344.0 ± 3.6	0.260 ± 0.088	0.334 ± 0.087	4.90 ± 0.53	6.11 ± 0.47	8.91 ± 0.06
(16:0)$_2$*P*(CH$_2$)$_{n3}$NMe$_3$ odd n_3[c]	329.8	0.394	0.422	−10.48[d]	−10.75[d]	7.60
even n_3[c]	317.7	0.032	0.029	−15.44[d]	−15.54[d]	6.00

Experimental data fitted are from refs. [72–77]. Except for the phosphatidyl trimethylalkanolamine series, (16:0)$_2$*P*(CH$_2$)$_{n3}$NMe$_3$ [77], the fits are those given previously in ref. [15]. In the latter reference, however, an alternative definition was used for the parameters $n_{3,H}$ and $n_{3,S}$.
[a] 2-(6:0)16:0: 2-hexylhexadecanoyl, etc.
[b] TPE: phosphatidylethanolamine prepared by transphosphatidylation of egg phosphatidylcholine.
[c] *P*(CH$_2$)$_5$NMe$_3$ is phosphatidyl trimethylpentanolamine, etc.; *P*(CH$_2$)$_2$NMe$_3$ ≡ PC.
[d] Note that $\Delta H_{inc,3}$ and $\Delta S_{inc,3}$ are also negative (see legend to Fig. 15 and Eqs. (19)–(21)).

well-packed chains. Interestingly, this is also close to the critical chain length below which phosphatidylcholines, and other diacyl phospholipids, do not form stable bilayers [71].

9. Length of zwitterionic head groups

Although not strictly pertaining to chain structure, phosphatidylcholine analogues exhibit a biphasic dependence of chain-melting enthalpy, entropy and transition temperature on separation between phosphate and quaternary nitrogen in the zwitterionic headgroup [77]. Fig. 15 shows the dependence of transition temperature, enthalpy and entropy on number, n_3, of CH_2 groups between phosphate and nitrogen in a homologous series of phosphatidyltrimethylalkanolamines. All calorimetric parameters display an odd–even alternation. This indicates that the headgroup conformation/orientation must differ between analogues with odd and even numbers of CH_2 groups separating the phosphate and nitrogen. For both odd and even analogues, the chain-melting properties have a biphasic dependence on headgroup length, n_3. The dependence of the transition enthalpy and entropy on n_3 is approximately bilinear with absolute slopes for the odd analogues that differ considerably above and below the critical length, $n_3 = \Delta n_3$, in accordance with Eqs. (19) and (20). In contrast to the headgroup-attached chains of Fig. 14, the chain-melting temperature goes through a maximum, rather than a minimum, with increasing length. Also, the variation with number of CH_2 groups is considerably smaller in total extent for the zwitterionic headgroups.

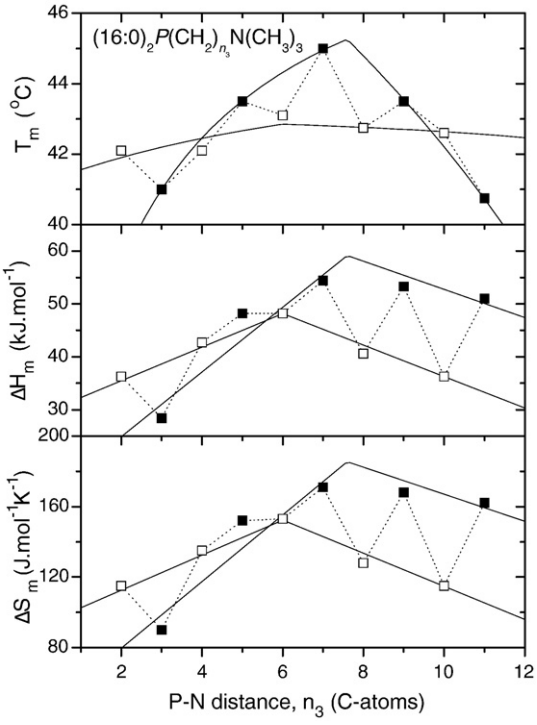

Fig. 15. Dependence of chain-melting transition temperature (top panel), transition enthalpy (middle panel), and transition entropy (bottom panel), on number of CH_2 groups, n_3, between the phosphate and quaternary nitrogen in the head group of 1,2-dipalmitoyl phosphatidyl-trimethylalkanolamines. Open symbols are for even values of n_3 and solid symbols are for odd values. Data from ref. [77]. Solid lines are predictions of Eq. (21) for the transition temperature (top panel) with the parameters given in Table 7, and of Eqs. (19), (20) for the transition enthalpy and entropy (middle and bottom panels) with the additional values of $\Delta H_{inc,3} = -4.39$ (−3.08) kJ mol^{-1} per CH_2 and $\Delta S_{inc,3} = -13.29$ (−9.69) J mol^{-1} K^{-1} per CH_2 for odd (even) values of n_3.

Unfortunately, the odd–even alternation effectively halves the available number of data points, and limits the resolution with which the critical headgroup length, Δn_3, can be determined. For the chain-melting temperature, the number of data points in the odd or even series is less than the number of parameters in Eq. (21). Nevertheless, the transition temperature, enthalpy and entropy for both odd and even series can be reasonably well described by Eqs. (19)–(21) with a consistent set of parameters. These simulations are given by the solid lines in Fig. 15, and the parameters are listed in Table 7 (with the additional values of $\Delta H_{inc,3}$ and $\Delta S_{inc,3}$ given in the legend to Fig. 15). It is notable that the variation in chain-melting temperature is considerably larger for the odd series than for the even series.

As proposed in ref. [77], the variation in chain-melting properties with head-group P-N distance in phosphatidyl trimethylalkanolamines probably reflects interactions between the phosphate and quaternary ammonium groups more than interactions of the linking chains *per se*. This is consistent with the odd–even alternation, which suggests that particular conformations are required to optimise interactions. Also, the critical P-N separation, Δn_3, at which this occurs differs between odd and even values of n_3. At chain lengths $n_3 < \Delta n_3$, headgroup conformations presumably are too restricted to allow optimum P-N interactions, whereas for $n_3 > \Delta n_3$, the linkage simply becomes too long and interactions more diffuse (cf. Fig. 15).

Interestingly, the chain-melting temperature of phosphatidylethanolamine analogues decreases with increasing number of CH_2 groups between phosphate and nitrogen [17,78,79]. The extent of variation is much greater than for the phosphatidylcholine analogues, presumably because hydrogen bonding in the PE head groups is disrupted. Data for the phosphatidylalkanolamine series are available only up to $n_3 = 5$, at which point the transition temperature is still decreasing rapidly.

10. Conclusion

The analysis of chain-melting in lipid membranes via systematic dependences of the chain-melting enthalpy and entropy on lipid structure (Eq. (2)) gives a rational, thermodynamically-based approach to describing the chain-melting temperatures. Linear dependences of the calorimetric properties on lipid chain length and on chain asymmetry have been demonstrated previously [14,17,38,80]. Examples for other structural parameters are given here. However, because transition temperatures can be determined with greater accuracy than can the other calorimetric quantities, better precision is obtained by fitting the resulting expressions for the transition temperatures (Eqs. 5, 8, 11, 14 and 21) directly.

Additional to previous treatments of several structural dependences, new analyses are developed here for mixed interdigitated gel phases of lipids with one chain twice the length of the other, for the positional dependence of chain methyl branches, for the dependence on head-group length of zwitterionic lipids, and for the chain asymmetry of sphingomyelins. This results in a detailed parameterization for many aspects of lipid molecular structure (Tables 1–7). The largest database is for phosphatidylcholines, but predictions for other species can be made from the differences between the end contributions (n_H and n_S) for the various symmetrical two-chain lipids that are given in Table 1. In this way one can begin to predict the chain-melting behaviour, and indirectly mixing properties, for many of the lipid species revealed by lipidomic surveys.

As already noted, these biophysical attributes of membrane lipids are essential to cellular function. A fluid membrane is needed not only for optimum cell growth, but also for the activity of membrane-bound enzymes and transport systems. The membrane phase state is crucial to such further lipid features as hydrophobic matching [7,81], membrane curvature stress [7,82], and transmembrane permeability barrier [83–85] that also are functionally significant. Last, but not least, is the involvement of sphingolipids in the formation of in-plane membrane domains: the dependence on chain asymmetry that is given here characterizes the influence of molecular structure on phase state for this important class of raft-forming membrane lipids.

References

[1] G.B. Warren, P.A. Toon, N.J. Birdsall, A.G. Lee, J.C. Metcalfe, Reversible lipid titrations of activity of pure adenosine triphosphatese lipid complexes, Biochemistry 13 (1974) 5501–5507.

[2] P. Fajer, P.F. Knowles, D. Marsh, Rotational motion of yeast cytochrome oxidase in phosphatidylcholine complexes studied by saturation-transfer electron spin resonance, Biochemistry 28 (1989) 5634–5643.

[3] P. Overath, L. Thilo, H. Träuble, Lipid phase transitions and membrane function, Trends Biochem. Sci. 1 (1976) 186–189.

[4] R.N. McElhaney, The relationship between membrane lipid fluidity and phase state and the ability of bacteria and mycoplasmas to grow and survive at various temperatures, in: M. Kates, L. Manson (Eds.), Biomembranes, Vol. 12, Academic Press, New York, 1984, pp. 249–278.

[5] R.N. McElhaney, Membrane lipid fluidity, phase state and membrane function in prokaryotic microorganisms, in: R.A. Aloia, J.M. Boggs (Eds.), Membrane fluidity in biology, 4, Academic Press, New York, 1985, pp. 147–208.

[6] R.N. McElhaney, The effect of membrane lipids on permeability and transport in prokaryotes, in: G. Benga (Ed.), Structure and properties of cell membranes, Vol. 2, CRC Press, Boca Raton FL, 1985, pp. 19–52.

[7] D. Marsh, Protein modulation of lipids, and *vice-versa*, in membranes, Biochim. Biophys. Acta 1778 (2008) 1545–1575.

[8] E.A. Evans, D. Needham, Physical properties of surfactant bilayer-membranes - thermal transitions, elasticity, rigidity, cohesion, and colloidal interactions, J. Phys. Chem. 91 (1987) 4219–4228.

[9] E.A. Evans, R. Skalak, Mechanics and Thermodynamics of Biomembranes, CRC Press, Boca Raton, FL, 1980.

[10] D. Marsh, Elastic curvature constants of lipid monolayers and bilayers, Chem. Phys. Lipids 144 (2006) 146–159.

[11] K. Simons, E. Ikonen, Functional rafts in cell membranes, Nature 387 (1997) 569–572.

[12] D. Marsh, Cholesterol-induced fluid membrane domains: a compendium of lipid-raft ternary phase diagrams, Biochim. Biophys. Acta 1788 (2009) 2114–2123.

[13] D. Marsh, Analysis of the chainlength dependence of lipid phase transition temperatures: main transitions and pretransitions of phosphatidylcholines; main and non-lamellar transitions of phosphatidylethanolamines, Biochim. Biophys. Acta 1062 (1991) 1–6.

[14] D. Marsh, Analysis of the bilayer phase transition temperatures of phosphatidylcholines with mixed chains, Biophys. J. 61 (1992) 1036–1040.

[15] D. Marsh, Chain-melting transition temperatures of phospholipids with acylated or alkylated headgroups (*N*-acyl phosphatidylethanolamines and *O*-alkyl phosphatidic acids), or with α-branched chains, Biochim. Biophys. Acta 1414 (1998) 249–254.

[16] D. Marsh, Thermodynamic analysis of chain-melting transition temperatures for monounsaturated phospholipid membranes: dependence on *cis*-monoenoic double bond position, Biophys. J. 77 (1999) 953–963.

[17] J.M. Seddon, G. Cevc, D. Marsh, Calorimetric studies of the gel-fluid (L_β-L_α) and lamellar-inverted hexagonal (L_α-H_{II}) phase transitions in dialkyl- and diacylphosphatidylethanolamines, Biochemistry 22 (1983) 1280–1289.

[18] R.N.A.H. Lewis, N. Mak, R.N. McElhaney, A differential scanning calorimetric study of the thermotropic phase behavior of model membranes composed of phosphatidylcholines containing linear saturated fatty acyl chains, Biochemistry 26 (1987) 6118–6126.

[19] T.G. Burke, A.S. Rudolph, R.R. Price, J.P. Sheridan, A.W. Dalziel, A. Singh, P.E. Sheen, Differential scanning calorimetric study of the thermotropic phase behavior of a polymerizable, tubule-forming lipid, Chem. Phys. Lipids 48 (1988) 215–230.

[20] G. Lipka, B.Z. Chowdhry, J.M. Sturtevant, A comparison of the phase transition properties of 1,2-diacylphosphatidylcholines and 1,2-diacylphosphatidylethanolamines in H_2O and D_2O, J. Phys. Chem. 88 (1984) 5401–5406.

[21] R.N.A.H. Lewis, R.N. McElhaney, Calorimetric and spectroscopic studies of the polymorphic phase behavior of a homologous series of *n*-saturated 1,2-diacyl phosphatidylethanolamines, Biophys. J. 64 (1993) 1081–1096.

[22] J.M. Seddon, G. Cevc, R.D. Kaye, D. Marsh, X-ray diffraction study of the polymorphism of hydrated diacyl- and dialkylphosphatidylethanolamines, Biochemistry 23 (1984) 2634–2644.

[23] Y.-P. Zhang, R.N.A.H. Lewis, R.N. McElhaney, Calorimetric and spectroscopic studies of the thermotropic phase behavior of the *n*-saturated 1,2-diacylphosphatidylglycerols, Biophys. J. 72 (1997) 779–793.

[24] R.N.A.H. Lewis, R.N. McElhaney, Calorimetric and spectroscopic studies of the thermotropic phase behavior of lipid bilayer model membranes composed of a homologous series of linear saturated phosphatidylserines, Biophys. J. 79 (2000) 2043–2055.

[25] R.A. Demel, C.C. Yin, B.Z. Lin, H. Hauser, Monolayer characteristics and thermal behavior of phosphatidic acids, Chem. Phys. Lipids 60 (1992) 209–223.

[26] R.N.A.H. Lewis, R.N. McElhaney, Thermotropic phase behavior of model membranes composed of phosphatidylcholines containing isobranched fatty acids. 1. Differential scanning calorimetric studies, Biochemistry 24 (1985) 2431–2439.

[27] C.P. Yang, M.C. Wiener, R.N.A.H. Lewis, R.N. McElhaney, J.F. Nagle, Dilatometric studies of isobranched phosphatidylcholines, Biochim. Biophys. Acta 863 (1986) 33–44.

[28] R.N.A.H. Lewis, B.D. Sykes, R.N. McElhaney, Thermotropic phase behavior of model membranes composed of phosphatidylcholines containing DL-methyl anteiso-branched fatty acids. 1. Differential scanning calorimetric and ^{31}P NMR spectroscopic studies, Biochemistry 26 (1987) 4036–4044.

[29] P. Nuhn, G. Brezesinski, B. Dobner, G. Förster, M. Gutheil, H.-D. Dörfler, Synthesis, calorimetry, and X-ray diffraction of lecithins containing branched fatty acid chains, Chem. Phys. Lipids 39 (1986) 221–236.

[30] R.N.A.H. Lewis, H.H. Mantsch, R.N. McElhaney, Thermotropic phase behavior of phosphatidylcholines with ω-tertiary-butyl fatty acyl chains, Biophys. J. 56 (1989) 183–193.

[31] R.N.A.H. Lewis, R.N. McElhaney, Thermotropic phase behavior of model membranes composed of phosphatidylcholines containing ω-cyclohexyl fatty acids—differential scanning calorimetric and ^{31}P NMR spectroscopic studies, Biochemistry 24 (1985) 4903–4911.

[32] H. Matsuki, E. Miyazaki, F. Sakano, N. Tamai, S. Kaneshina, Thermotropic and barotropic phase transitions in bilayer membranes of ether-linked phospholipids with varying alkyl chain lengths, Biochim. Biophys. Acta 1768 (2007) 479–489.

[33] R.N.A.H. Lewis, D.A. Mannock, R.N. McElhaney, D.C. Turner, S.M. Gruner, Effect of fatty acyl chain length and structure on the lamellar gel to liquid crystalline and lamellar to reversed hexagonal phase transitions of aqueous phosphatidylethanolamine dispersions, Biochemistry 28 (1989) 541–548.

[34] H. Xu, F.A. Stephenson, H. Lin, C.H. Huang, Phase metastability and supercooled metastable state of diundecanoylphosphatidylethanolamine bilayers, Biochim. Biophys. Acta 943 (1988) 63–75.

[35] R.B. Sisk, C. Huang, Calorimetric studies on the influence of N-methylated headgroups on the mixing behavior of diheptadecanoyl phopshatidylcholine with 1-behenoyl-2-lauroylphosphatidylcholine, Biophys. J. 61 (1992) 593–603.

[36] J. Gagné, L. Stamatatos, T. Diacovo, S.-W. Hui, P.L. Yeagle, J.R. Silvius, Physical properties and surface interactions of bilayer membranes containing *N*-methylated phosphatidylethanolamines, Biochemistry 24 (1985) 4400–4408.

[37] B.Z. Chowdhry, A.W. Dalziel, Phase transition properties of 1,2-diacylphosphatidylethanolamines and 1,3-diacylphosphatidylethanolamines with modified head groups, Biochemistry 24 (1985) 4109–4117.

[38] M.J. Swamy, D. Marsh, M. Ramakrishnan, Differential scanning calorimetry of chain-melting phase transitions of *N*-acylphosphatidylethanolamines, Biophys. J. 73 (1997) 2556–2564.

[39] D.A. Mannock, R.N.A.H. Lewis, R.N. McElhaney, Physical properties of glycosyl diacylglycerols. 1. Calorimetric studies of a homologous series of 1,2-di-O-acyl-3-O-(α-D-glucopyranosyl)-*sn*-glycerols, Biochemistry 29 (1990) 7790–7799.

[40] D.A. Mannock, R.N.A.H. Lewis, A. Sen, R.N. McElhaney, The physical properties of glycosyldiacylglycerols. Calorimetric studies of a homologous series of 1,2-di-O-acyl-3-O-(β-D-glucopyranosyl)-*sn*-glycerols, Biochemistry 27 (1988) 6852–6859.
[41] D.A. Mannock, R.N. McElhaney, Differential scanning calorimetry and x-ray diffraction studies of a series of synthetic β-D-galactosyl diacylglycerols, Can J. Biochem. Cell Biol. 69 (1991) 863–867.
[42] H.-J. Hinz, H.L. Kuttenreich, R. Meyer, M. Renner, R. Fründ, R. Koynova, A.I. Boyanov, B.G. Tenchov, Stereochemistry and size of sugar head groups determine structure and phase behavior of glycolipid membranes—densitometric, calorimetic, and x-ray studies, Biochemistry 30 (1991) 5125–5138.
[43] H.L. Kuttenreich, H.-J. Hinz, R. Inczedy-Marcsek, R. Koynova, B. Tenchov, P. Laggner, Polymorphism of synthetic 1,2-O-dialkyl-3-O-β-D-galactosyl-*sn*-glycerols of different alkyl chain lengths, Chem. Phys. Lipids 47 (1988) 245–260.
[44] H. Lin, Z. Wang, C. Huang, Differential scanning calorimetry study of mixed-chain phosphatidylcholines with a common molecular weight identical with diheptadecanoylphosphatidylcholine, Biochemistry 29 (1990) 7063–7072.
[45] H.N. Lin, Z.Q. Wang, C.H. Huang, The influence of acyl chain-length asymmetry on the phase transition parameters of phosphatidylcholine dispersions, Biochim. Biophys. Acta 1067 (1991) 17–28.
[46] I. Pascher, M. Lundmark, P.-G. Nyholm, S. Sundell, Crystal structures of membrane lipids, Biochim. Biophys. Acta 1113 (1992) 339–373.
[47] D. Marsh, T. Páli, Lipid conformation in crystalline bilayers and in crystals of transmembrane proteins, Chem. Phys. Lipids 141 (2006) 48–65.
[48] T. Bultmann, H. Lin, Z. Wang, C. Huang, Thermotropic and mixing behavior of mixed-chain phosphatidylcholines with molecular weights identical with that of L-α-dipalmitoylphosphatidylcholine, Biochemistry 30 (1991) 7194–7202.
[49] R.V. Durvasula, C. Huang, Thermotropic phase behavior of mixed-chain phosphatidylglycerols: implications for acyl chain packing in fully hydrated bilayers, Biochim. Biophys. Acta 1417 (1999) 111–121.
[50] P.K. Sripada, P.R. Maulik, J.A. Hamilton, G.G. Shipley, Partial synthesis and properties of *N*-acyl sphingomyelins, J. Lipid Res. 28 (1987) 710–718.
[51] Z. Wang, H. Lin, C. Huang, Differential scanning calorimetric study of a homologous series of fully hydrated saturated mixed-chain C(X):C(X+6) phosphatidylcholines, Biochemistry 29 (1990) 7072–7076.
[52] C. Huang, Empirical estimation of the gel to liquid crystalline phase-transition temperatures for fully hydrated saturated phosphatidylcholines, Biochemistry 30 (1991) 26–30.
[53] J.T. Mason, F.A. Stephenson, Thermotropic properties of saturated mixed acyl phosphatidylethanolamines, Biochemistry 29 (1990) 590–598.
[54] C. Huang, H. Lin, S. Li, G. Wang, Influence of the positions of *cis* double bonds in the *sn*-2-acyl chain of phosphatidylethanolamine on the bilayer's melting behavior, J. Biol. Chem. 272 (1997) 21917–21926.
[55] H. Lin, S. Li, G. Wang, E.E. Brumbaugh, C. Huang, A calorimetric study of binary mixtures of saturated and monounsaturated mixed-chain phosphatidylethanolamines, Biochim. Biophys. Acta 1283 (1996) 199–206.
[56] A. Blume, in: C. Hidalgo (Ed.), Physical properties of biological membranes and their functional implications, Plenum Press, New York, 1988, p. 71.
[57] R.H. Pearson, I. Pascher, The molecular structure of lecithin dihydrate, Nature (Lond.) 281 (1979) 499–501.
[58] G. Zaccai, G. Büldt, A. Seelig, J. Seelig, Neutron diffraction studies on phosphatidylcholine model membranes. II. Chain conformation and segmental disorder, J. Mol. Biol. 134 (1979) 693–706.
[59] J.T. Mason, C.-H. Huang, R.L. Biltonen, Calorimetric investigations of saturated mixed-chain phosphatidylcholine bilayer dispersions, Biochemistry 20 (1981) 6086–6092.
[60] C. Huang, Z.Q. Wang, H.N. Lin, E.E. Brumbaugh, S.S. Li, Calorimetric studies of fully hydrated phosphatidylcholines with highly asymmetric acyl chains, Biochim. Biophys. Acta 1145 (1993) 298–310.
[61] R.N.A.H. Lewis, R.N. McElhaney, R. Osterberg, S.M. Gruner, Enigmatic thermotropic phase behavior of highly asymmetric mixed-chain phosphatidylcholines that form mixed interdigitated gel phases, Biophys. J. 66 (1994) 207–216.
[62] J. Shah, P.K. Sripada, G.G. Shipley, Structure and properties of mixed-chain phosphatidylcholine bilayers, Biochemistry 29 (1990) 4254–4262.
[63] P.G. Barton, F.D. Gunstone, Hydrocarbon chain packing and molecular motion in phospholipid bilayers formed from unsaturated lecithins, J. Biol. Chem. 250 (1975) 4470–4476.
[64] Z. Wang, H. Lin, S. Li, C. Huang, Phase transition behavior and molecular structures of monounsaturated phosphatidylcholines, J. Biol. Chem. 270 (1995) 2014–2023.
[65] G. Wang, H. Lin, S. Li, C. Huang, Phosphatidylcholines with *sn*-1 saturated and *sn*-2 *cis*-monounsaturated acyl chains, J. Biol. Chem. 270 (1995) 22738–22746.
[66] C.J. Dekker, W.S.M. Guerts van Kessel, J.P.G. Klomp, J. Pieters, B. de Kruijff, Synthesis and polymorphic phase behaviour of polyunsaturated phosphatidylcholines and phosphatidylethanolamines, Chem. Phys. Lipids 33 (1983) 93–106.
[67] C. Huang, Z.Q. Wang, H.N. Lin, E.E. Brumbaugh, S.S. Li, Interconversion of bilayer phase transition temperatures between phosphatidylethanolamines and phosphatidylcholines, Biochim. Biophys. Acta 1189 (1994) 7–12.
[68] C. Huang, S. Li, H. Lin, G. Wang, On the bilayer phase transition temperatures for monoenoic phosphatidylcholines and phosphatidylethanolamines and the interconversion between them, Arch. Biochem. Biophys. 334 (1996) 135–142.
[69] Z. Wang, H. Lin, S. Li, C. Huang, Calorimetric studies and molecular mechanics simulations of monounsaturated phosphatidylethanolamine bilayers, J. Biol. Chem. 269 (1994) 23491–23499.
[70] M.J. Swamy, M. Ramakrishnan, B. Angerstein, D. Marsh, Spin-label electron spin resonance studies on the mode of anchoring and vertical location of the *N*-acyl chain in *N*-acylphosphatidylethanolamines, Biochemistry 39 (2000) 12476–12484.
[71] J.H. Kleinschmidt, L.K. Tamm, Structural transitions in short-chain lipid assemblies studied by ^{31}P NMR spectroscopy, Biophys. J. 83 (2002) 994–1003.
[72] G. Brezesinski, B. Dobner, H.-D. Dörfler, M. Fischer, S. Haas, P. Nuhn, Influence of α-branched fatty acid chains on the thermotropic behaviour of 1-*O*-acyl-2-*O*-hexadecyl-glycerophosphocholines, Chem. Phys. Lipids 43 (1987) 257–264.
[73] H. Eibl, Phospholipid bilayers: influence of structure and charge, in: W.H. Kunau, R.T. Holman (Eds.), Polyunsaturated Fatty Acids, American Oil Chemists' Society, Champaign, IL, 1977, pp. 229–244.
[74] J.C. Domingo, M. Mora, M.A. de Madariaga, The influence of *N*-acyl chain length on the phase behaviour of natural and synthetic *N*-acylethanolamine phospholipids, Chem. Phys. Lipids 75 (1995) 15–25.
[75] S. Akoka, C. Tellier, C. Le Roux, D. Marion, A phosphorus magnetic resonance spectroscopy and a differential scanning calorimetry study of the physical properties of *N*-acylphosphatidylethanolamines in aqueous dispersions, Chem. Phys. Lipids 46 (1988) 43–50.
[76] D. Lafrance, D. Marion, M. Pézolet, Study of the structure of *N*-acyldipalmitoylphosphatidylethanolamines in aqueous dispersion by infrared and Raman spectroscopies, Biochemistry 29 (1990) 4592–4599.
[77] D. Bach, I. Bursuker, H. Eibl, I.R. Miller, Differential scanning calorimetry of dipalmitoyl phosphatidylcholine analogs and of their interaction products with basic polypeptides, Biochim. Biophys. Acta 514 (1978) 310.
[78] R. Leventis, N. Fuller, R.P. Rand, P.L. Yeagle, A. Sen, M.J. Zuckerman, J.R. Silvius, Molecular organization and stability of hydrated dispersions of headgroup-modified phosphatidylethanolamine analogues, Biochemistry 30 (1991) 7212–7219.
[79] J.R. Silvius, P.M. Brown, T.L. O'Leary, Role of head group structure in the phase behavior of amino phospholipids. 1. Hydrated and dehydrated lamellar phases of saturated phosphatidylethanolamine analogues, Biochemistry 25 (1986) 4249–4258.
[80] M.J. Swamy, B. Angerstein, D. Marsh, Differential scanning calorimetry of thermotropic phase transitions in vitaminylated lipids: aqueous dispersions of *N*-biotinyl phosphatidylethanolamines, Biophys. J. 66 (1994) 31–39.
[81] D. Marsh, Energetics of hydrophobic matching in lipid-protein interactions, Biophys. J. 94 (2008) 3996–4013.
[82] D. Marsh, Lateral pressure profile, spontaneous curvature frustration, and the incorporation and conformation of proteins in membranes. Biophys. J. 93 (2007) 3884–3899.
[83] D. Marsh, Polarity and permeation profiles in lipid membranes, Proc. Natl. Acad. Sci. U. S. A. 98 (2001) 7777–7782.
[84] D.A. Erilov, R. Bartucci, R. Guzzi, A.A. Shubin, A.G. Maryasov, D. Marsh, S.A. Dzuba, L. Sportelli, Water concentration profiles in membranes measured by ESEEM of spin-labeled lipids, J. Phys. Chem. B 109 (2005) 12003–12013.
[85] D. Kurad, G. Jeschke, D. Marsh, Lipid membrane polarity profiles by high-field EPR, Biophys. J. 85 (2003) 1025–1033.
[86] D.A. Mannock, R.N.A.H. Lewis, R.N. McElhaney, P.E. Harper, D.C. Turner, S.M. Gruner, An analysis of the relationship between fatty acid composition and the lamellar gel to liquid-crystalline and the lamellar to inverted nonlamellar phase transition temperatures of phosphatidylethanolamines and diacyl-D-glucosyl glycerols, Eur. Biophys. J. 30 (2001) 537–554.
[87] D.A. Mannock, M. Akiyama, R.N.A.H. Lewis, R.N. McElhaney, Synthesis and thermotropic characterization of a homologous series of racemic β-D-glucosyl dialkylglycerols, Biochim. Biophys. Acta 1509 (2000) 203–215.
[88] D.A. Mannock, M.D. Collins, M. Kreichbaum, P.E. Harper, S.M. Gruner, R.N. McElhaney, The thermotropic phase behaviour and phase structure of a homologous series of racemic β-D-galactosyl dialkylglycerols studied by differential scanning calorimetry and X-ray diffraction, Chem. Phys. Lipids 148 (2007) 26–50.